Characterizing the fluctuations of dynamic resting-state electrophysiological functional connectivity: Reduced neuronal coupling variability in mild cognitive impairment and dementia due to Alzheimer's disease

Pablo Núñez[1], Jesús Poza[1,2,3], Carlos Gómez[1], Víctor Rodríguez-González[1], Arjan Hillebrand[4], Miguel A. Tola-Arribas[5], Mónica Cano[6], Roberto Hornero[1,2,3]

[1] Biomedical Engineering Group, University of Valladolid, Valladolid, Spain
[2] IMUVA, Instituto de Investigación en Matemáticas, University of Valladolid, Spain
[3] INCYL, Instituto de Neurociencias de Castilla y León, Salamanca, Spain
[4] Department of Clinical Neurophysiology and MEG Center, Amsterdam UMC, Vrije Universiteit Amsterdam, Amsterdam Neuroscience, Amsterdam, The Netherlands
[5] Department of Neurology, Río Hortega University Hospital, Valladolid, Spain
[6] Department of Clinical Neurophysiology, Río Hortega University Hospital, Valladolid, Spain

E-mail: `pablo.nunez@gib.tel.uva.es`

Abstract. *Objective.* The characterization of brain functional connectivity is a helpful tool in the study of the neuronal substrates and mechanisms that are altered in Azheimer's Disease (AD) and mild cognitive impairment (MCI). Recently, there has been a shift towards the characterization of dynamic functional connectivity (dFC), discarding the assumption of connectivity stationarity during the resting-state. The majority of these studies have been performed with functional magnetic resonance imaging (fMRI) recordings, with only a small subset being based on magnetoencephalography/electroencephalography (MEG/EEG). However, only these modalities enable the characterization of potentially fast brain dynamics, which is mandatory for an accurate understanding of the transmission and processing of neuronal information. The aim of this study was to characterize the dFC of resting-state EEG activity in AD and MCI. *Approach.* Three measures: the phase lag index (PLI), leakage-corrected magnitude squared coherence (MSCOH) and leakage-corrected amplitude envelope correlation (AEC) were computed for 45 patients with dementia due to AD, 51 subjects with MCI due to AD and 36 cognitively healthy controls. All measures were estimated in epochs of 60 s using a sliding window approach. An epoch length of 15 s was used to provide reliable results. We tested whether the observed PLI, MSCOH and AEC fluctuations reflected actual variations in functional connectivity, as well as whether between-group differences could be found. *Main results.* We found dFC using PLI, MSCOH and AEC, with AEC having the highest number of statistically significant connections, followed by MSCOH and PLI. Furthermore, a significant reduction in AEC dFC for patients with AD compared to controls was found in the alpha (8-13 Hz) and beta-1 (13-30 Hz) bands. *Significance.* Our results suggest that patients with AD (and MCI subjects to a lesser degree) show less variation in neuronal connectivity during resting-state, supporting the notion that dFC can be found at the EEG time scale

and is abnormal in the MCI-AD continuum. Measures of dFC have the potential of being used as biomarkers of AD. Moreover, they could also suggest that AD resting-state networks may operate at a state of low firing activity induced by the observed reduction in coupling strength. Furthermore, the statistically significant correlation between dFC and relative power in the beta-1 band could be related to pathologically high levels of neural activity inducing a loss of dFC. These findings show that the stability of neuronal coupling is affected in AD and MCI.

Keywords: Alzheimer's disease, mild cognitive impairment, dynamic functional connectivity, electroencephalography, phase lag index, coherence, amplitude envelope correlation

Submitted to: *J. Neural Eng.*

1. Introduction

The human brain is a complex system composed of neurons connected through an intricate network of synapses [1]. The behavior of the brain during resting-state has been widely studied with a variety of techniques, such as functional magnetic resonance imaging (fMRI), magnetoencephalography (MEG), electroencephalography (EEG) and positron emission tomography (PET) [2]. Until recently, the majority of studies assumed that the statistical interdependence between distinct brain regions (functional connectivity, FC [3, 4]) remains temporally stationary during resting-state, and is therefore refered to as *static functional connectivity* (sFC) [2, 5].

While sFC studies have offered insights into the neurophysiological properties of the brain, it has been proposed that the brain does not remain in a state of equilibrium during the resting-state, but instead shows fluctuating connectivity patterns [6], referred to as *dynamic functional connectivity* (dFC). Thus, the quantification of these dynamic changes in FC metrics could provide relevant information into the properties of brain networks [2]. The vast majority of dFC studies have been performed with fMRI recordings, which is also the most widespread method in sFC studies, and different studies have shown transitions switching between discrete FC states on the scale of seconds to minutes [2, 6, 7, 8].

However, EEG is a cost-effective tool that is widely used in clinical settings, and which directly measures the electrical activity generated by synchronized neuronal firing of cortical neurons [9], providing information on neuronal coupling. In contrast to fMRI, EEG has a high temporal resolution due to its high sampling rate, which is useful for the characterization of spontaneous oscillatory activity in the cortex [1], and enables direct assessment of fast fluctuations in neuronal connectivity that fMRI may obfuscate [10]. Furthermore, the low cost of EEG over other imaging methods makes it more readily available in clinical environments. Concurrent EEG and fMRI recordings have been used to characterize the correlation between dynamic fMRI connectivity states and the locally activated EEG power spectra [7, 11, 12], as well as the microstates observable on EEG scalp topography [13]. A study performed using EEG data recorded during a task-free paradigm quantified the dynamics of network measures using a sliding window approach [14], revealing the existence of a core network formed by a set of brain regions that may dynamically play the role of local or global hubs. Another study used MEG imaging to characterize the dynamic FC of hub load in patients before and 1-year after undergoing lesion resection [15]. The characterization of dFC in patients with neurological disorders could be used to discover possible alterations caused by the disorder. This could help to better understand the neuronal substrates and select appropriate therapies for patients.

One neurodegenerative disorder that could benefit from EEG dFC studies is dementia due to Alzheimer's disease (AD). AD is a neurodegenerative disorder that progressively extends over different brain areas as it advances [16], disrupting the neuronal networks and producing aberrant connectivity patterns in, and between, neuronal circuits [17]. In particular, numerous resting-state EEG studies point to abnormal static coupling in AD that becomes more marked as the disease progresses[18, 19]. Accumulating evidence suggests that AD is a disconnection syndrome: a disruption in the spatio-temporal FC among different brain regions that underlies cognitive impairment [20]. Previous studies have found dFC in fMRI to be altered in patients with AD with respect to healthy controls, with differences in dwell time in default mode network (DMN) sub-network configurations. In particular, AD subjects had longer dwell time in anterior DMN configurations and less in posterior DMN configurations when compared to controls [21]. Thus, studying the temporal features of AD FC on the faster EEG time scale may also help with better characterization of the disease. Moreover, mild cognitive impairment (MCI) is defined as an early state of cognitive impairment, which can be considered a prodromal state of AD [22]. It has been found that MCI subjects show subtle neuronal coupling abnormalities compared to healthy elderly controls [9, 23, 24, 25]. Many MCI patients progress to AD at a later stage [22], making it essential to accurately characterize MCI-related neuronal coupling abnormalities in order to provide an early AD or MCI diagnosis.

In a preliminary work, we applied a statistical method, previously used to detect dFC in fMRI [5], to EEG recordings. We found that the variability in EEG functional connectivity during 60 second trials, measured by means of magnitude squared coherence (MSCOH), could be interpreted as dFC for both healthy subjects and patients with AD [26]. In the present study, we aimed to expand on this work by addressing some of its limitations, such as the absence of leakage correction and normalization for between-group comparisons, as well as the absence of an MCI group.

The main hypothesis of this paper was that the fMRI dFC patterns observable in healthy controls, MCI patients and patients with AD reflect dynamic behavior in the cerebral system, and that these dFC patterns can also be found at the EEG time scale. Furthermore, these patterns might be altered in MCI

and AD: we speculated that there might be a deficit in dFC in MCI and AD patients that is related to altered switching of the normal resting-state network configurations [27]. Specifically, the aim of this study is to address the following research questions: (i) what epoch length is needed to obtain an estimation of dFC?; (ii) can dFC be found in AD and MCI patients, as well as healthy controls?; (iii) do dFC patterns differ between groups?

2. Materials

2.1. Subjects

The study sample was formed by 132 subjects: 45 patients with dementia due to AD, 51 patients with MCI due to AD and 36 cognitively healthy controls. Patients with MCI or dementia due to AD were diagnosed according to the criteria of the National Institute on Aging and Alzheimer's Association (NIA-AA) [28, 29]. The control group was composed of elderly subjects with no history of neurological or psychiatric disorders. Potential subjects were excluded according to the following exclusion criteria: (1) presence or history of another neurological or psychiatric disease; (2) atypical course or uncommon clinical presentations according to the NIA-AA criteria; (3) advanced dementia (Clinical Dementia Rating = 3); (4) institutionalized patients; (5) medication that could influence EEG activity. The socio-demographic characteristics of each group are specified in Table 1.

All participants and caregivers were informed about the research and study protocol and gave their written informed consent. The Ethics Committee of the Río Hortega University Hospital (Valladolid, Spain) approved the study according to the Code of Ethics of the World Medical Association (Declaration of Helsinki).

2.2. Electroencephalographic recordings

EEG signals were recorded using a 19-channel EEG system (XLTEK®, Natus Medical) at the Department of Clinical Neurophysiology of the Río Hortega University Hospital, Valladolid, Spain. EEG activity was recorded according to the specifications of the international 10-20 system from Fp1, Fp2, Fz, F3, F4, F7, F8, Cz, C3, C4, T3, T4, T5, T6, Pz, P3, P4, O1, and O2, at a sampling frequency of 200 Hz. The recorded signals were bipolar and common average referencing (CAR) was chosen as the reference technique. Subjects were asked to remain with eyes closed, awake, and still during EEG acquisition. In order to prevent sleepiness, EEG traces were visually monitored on real time and if signs of drowsiness were found, subjects were asked to remain awake. Eye-movement related artifacts, drowsiness episodes, and subtle muscle activity were identified and marked during EEG recordings.

Five minutes of EEG activity were recorded for each subject, which was then preprocessed in four steps: (i) preliminary independent component analysis to remove components with artifacts; (ii) FIR filtering (Hamming window, filter order 2000, forward and backward filtering) to remove 50 Hz noise power and to limit spectral content to the wide frequency band of [1 70] Hz; and (iii) visual rejection of remaining artifacts, selecting the first 60 consecutive seconds without artifacts for each subject.

3. Methods

3.1. Estimation of connectivity

There are a variety of methods that can be used to characterize the functional connectivity between the EEG signals from two channels [30]. In this study, we characterized EEG dFC by means of three different connectivity measures: phase lag index (PLI), MSCOH and amplitude envelope correlation (AEC). PLI is a purely phase-based measure [31], MSCOH combines sensitivity to phase and amplitude synchrony (although it is more influenced by phase relationships [30]), and AEC is an amplitude-based measure [32]. PLI and MSCOH have been widely used in FC studies [33, 18], while leakage corrected AEC has been recommended for use due to its consistency [34]. These approaches represent fundamentally different underlying physiological processes [35].

3.1.1. Phase lag index The PLI evaluates the asymmetry of the distribution of instantaneous phase differences between time series [31]. PLI is defined as:

$$PLI = |\langle sign[\sin(\Delta\phi(t_k))]\rangle| \quad (1)$$

where $\Delta\phi(t_k)$ is a time series of phase differences between two channels. The PLI lies in the range of 0 and 1, with zero indicating that there is no coupling or coupling with zero-phase lag (volume conduction, or true zero-lag coupling) and 1 indicating perfect non-zero lag phase coupling [31]. The main advantage of the PLI over other connectivity measures is that it is insensitive to the effects of volume conduction [31].

3.1.2. Magnitude squared coherence Coherency is defined as the standardized cross-spectrum of two complex time series X and Y, standardized by dividing the cross-spectrum by the square root of the power spectrum of each time series [30]. The absolute value

Table 1. Socio-demographic and clinical data. AD: Alzheimer's disease; MCI: mild cognitive impairment; m: median; IQR: interquartile range ; M: male; F: female; A: primary education or below; B: secondary education or above; MMSE: Mini-Mental State Examination.

Data	Group		
	Patients with AD	MCI subjects	Controls
Number of subjects	45	51	36
Age (years) (m[IQR])	79.50[74.70, 82.40]	77.2[69.6, 79.75]	75.9[74.12, 78.62]
Sex (M:F)	20 : 25	21 : 30	11 : 25
Education level (A:B)	31 : 14	35 : 16	11 : 25
MMSE (m[IQR])	22[20, 24]	27[26, 28]	29[28, 30]

of coherency, which is a complex number, is known as coherence (COH):

$$COH_{xy}(f) = \frac{|S_{XY}(f)|}{\sqrt{P_X(f)P_Y(f)}} \quad (2)$$

where S_{XY} is the cross-spectrum of signals X and Y, and P_X and P_Y are their respective power spectra.

Coherence can be interpreted as the amount of variance in one signal that can be explained by the other, or vice-versa [33]. MSCOH is the squared value of coherence:

$$MSCOH_{xy}(f) = \frac{|S_{XY}(f)|^2}{P_X(f)P_Y(f)} \quad (3)$$

As previously stated, MSCOH is primarily influenced by phase synchrony and can be considered as a measure of the consistency of phase differences between two signals weighted by their magnitudes [30]. The time series were orthogonalized for each time-window separately before computing MSCOH in order to eliminate correlations due to field spread or volume conduction [10].

3.1.3. Amplitude envelope correlation AEC characterizes the correlation of the magnitudes of two time series for each frequency of interest. As opposed to MSCOH, AEC values can be high even when phase differences are randomly distributed [30]. AEC can be calculated by first band pass filtering the time series to the frequency band of interest. Then, the power envelope of each signal is obtained by means of the absolute value of the analytic signal, which is computed using the Hilbert transform. Finally, connectivity is calculated by computing the Pearson correlation between the log transformed power envelopes [36]. Again, in order to eliminate correlations due to field spread or volume conduction, the time series were orthogonalized for each time-window separately before computing the AEC [10].

3.1.4. Relative power Relative power (RP) is a measure used to describe the distribution of the spectral content of a signal. RP quantifies the relative contribution of different frequency bands to the global power spectrum. For each frequency band, RP is computed by summing the contribution of each spectral component in that specific band [37]. In the current study, RP was computed from the power spectral density (PSD) in order to assess its relationship with the dFC measures:

$$RP_{band} = \sum_{f \in f_{band}} PSD(f) \quad (4)$$

where f_{band} refers to the range of frequencies in specific band. It is worth mentioning that the PSD needs to be normalized before computation of the RP so that the sum of RP in all bands is 1. In the present study, the PSD was normalized in the 1-30 Hz frequency range and computed for each individual electrode.

3.2. Detection of dynamic functional connectivity

It is important to take into account that the mere presence of fluctuations in the connectivity measures is not sufficient proof for the existence of dFC. Due to the noisy nature of the recordings, the fact that the observed values are estimates of the *true* values cannot be ignored [5]. Therefore, in order to determine whether the fluctuations observed reflect real dynamic FC, an appropriate statistical test must be carried out [5]. One such method, recommended due to its ease of use in practice [5], consists in the construction of N *surrogate* versions of the original signals. Then, the same connectivity measures are computed on the surrogate signals. Afterwards, one must determine whether the observed value of a *test statistic* obtained with the original signal has a statistically significant z-value with respect to the distribution of values of the same test statistic obtained with the surrogate versions of the signals [5]. In the present study, the standard deviations of PLI, MSCOH and AEC (κ_{PLI}, κ_{MSCOH} and κ_{AEC}) were used as test statistic [5].

It is very important that the surrogate versions of the original signals are constructed under an appropriate null hypothesis. The surrogate data must share all statistical properties with the original data, apart from the property one wants to test for.

In the case of detecting dFC, the surrogate signals must preserve sFC but lack dFC [5]. This way, the alternative hypothesis is that there is dFC, while the null hypothesis is that the FC is static. In the present study, surrogate versions of each EEG segment were constructed from the original signals using the amplitude adjusted Fourier transform (AAFT) method [38]. This method of constructing surrogate time series improves on the phase randomization method of constructing surrogate data [39] by retaining the amplitude distribution of the original time series [40]. Most importantly, the phase of all EEG channels has to be altered equally at each time point, but randomly over time so that sFC is maintained but dFC is destroyed [5, 40].

The aforementioned procedure was performed for all 19 EEG channels, that is, the phase structure was altered equally for every channel. Following the approach used by Hindriks *et al.*, 500 surrogate versions of each EEG segment were created to test whether the fluctuations in FC reflected dFC [5].

3.3. Protocol

In order to study the dynamic properties of functional connectivity coupling patterns, PLI, MSCOH and AEC were computed between each pair of electrodes over the 60 second epochs by means of a sliding window technique with 50 % overlap between epochs. However, we computed both measures for non-overlapping epochs as well to assess its possible influence on the results (see supplementary material). Afterwards, for each measure, the mean (μ_{PLI}, μ_{MSCOH} and μ_{AEC}) and the standard deviation (κ_{PLI}, κ_{MSCOH} and κ_{AEC}) were obtained. The standard deviation (κ) was used as the test statistic to detect the existence of dFC [5]. The connectivity matrices were computed in the conventional frequency bands: delta (δ, 1-4 Hz), theta (θ, 4-8 Hz), alpha (α, 8-13 Hz), beta-1 (β1, 13-19 Hz) and beta-2 (β2, 19-30 Hz). A statistical test was performed to detect connections with statistically significant κ (i.e. connections with evidence of dFC). Then, the matrices were grouped into five regions (frontal, left-temporal, right-temporal, central and parieto-occipital) to reduce the number of comparisons [41]. Afterwards, inter-regional and intra-regional mean (μ) and standard deviation (κ) values for all connections were averaged among the electrodes within each region pair. Figure 1 shows which EEG channels correspond to each region. This procedure resulted in a 5 x 5 connectivity matrix for each of the 5 frequency bands. All subsequent analyses were performed on these matrices. This protocol was performed in the aforementioned 5 conventional frequency bands.

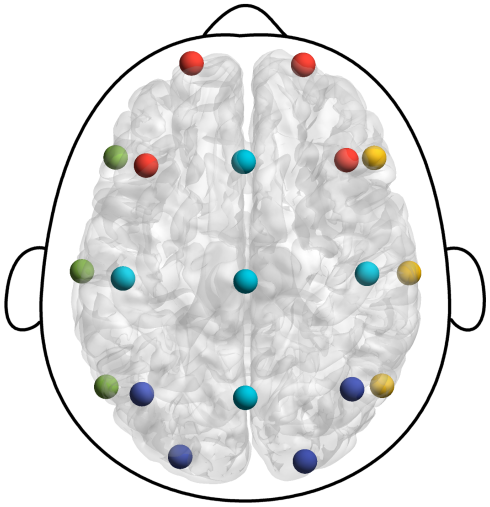

Figure 1. Correspondence between EEG channels and brain regions: frontal (red), central (light blue), right-temporal (yellow), left-temporal (green) and parieto-occipital (dark blue). Please note that the electrodes are located according to the international 10-20 system and visualized with the BrainNet Viewer (http://www. nitrc.org/projects/bnv/) [42].

3.4. Stability of the connectivity measures

It has been shown that FC metrics are biased by epoch length, with this bias being different for each metric [43]. To prevent a bias in the connectivity measures, we followed a procedure to detect the effect of different epoch lengths that has been used in resting-state EEG analyses on FC measures [43]. The epoch lengths were 1, 2, 3, 5, 10, 15 and 20 s, as these window sizes ensured that no part of the 60 second epoch was discarded. Friedman tests were performed to detect the effect of epoch length on FC measures. If the Friedman test showed a significant effect, the shortest epoch length that did not show statistically significant differences with any longer epoch (using Dunn's multiple comparison tests) was chosen as the shortest stable length [43]. This procedure was performed on the mean μ_{PLI}, μ_{MSCOH} and μ_{AEC} over all electrode pairs for each frequency band. The shortest epoch length deemed as stable for PLI, MSCOH and AEC was chosen for all further statistical analyses.

3.5. Statistical analyses

To perform between-group comparisons, all κ_{PLI}, κ_{MSCOH} and κ_{AEC} values for each subject were normalized by dividing them by the average κ values of their surrogate time series. This way, higher κ values that are not due to dFC, as well as lower κ values that can be explained by dFC, are corrected. By normalizing we can quantify how "dynamic"

each connection is, thus being able to compare all connections (not just those with statistically significant high κ) for every subject.

An exploratory analysis was carried out to assess the distribution of κ_{PLI}, κ_{MSCOH} and κ_{AEC} values. Normality was assessed with the Shapiro-Wilk test and homoscedasticity with the Levene test. The results showed that κ_{PLI}, κ_{MSCOH} and κ_{AEC} values did not meet parametric tests conditions. Thus, between-group differences were assessed with non-parametric tests.

Kruskal-Wallis tests were performed on the grand-average (average of all connections) κ_{PLI}, κ_{MSCOH} and κ_{AEC} values in each frequency band to detect global interactions between the three groups. If statistically significant between-group differences were found, permutation tests were performed to assess spatial pairwise between-group differences for the κ and μ of that connectivity measure in those frequency bands.

To control for type I error, false discovery rate (FDR) correction was used [44]. Thus, FDR correction for the number of connections was applied to control for the number of connections between regions, with a significance level of $\alpha = 0.05$. Signal processing was carried out using Matlab (version R2017a Mathworks, Natick, MA). The brain networks were visualized with the BrainNet Viewer (http://www. nitrc.org/projects/bnv/) [42].

4. Results

4.1. Comparison of patient characteristics

Statistical analyses were performed to assess possible differences between groups that might act as confounding factors. Subjects were matched by age ($\chi^2(2) = 5.41$, $p = 0.0670$, Kruskal-Wallis test) and sex ($\chi^2(2) = 1.72$, $p = 0.4217$, Chi-squared test). They were not, however, matched by education level ($\chi^2(2) = 15.71$, $p = 0.0004$, Chi-squared test). In order to test whether this mismatch could affect the between-group comparisons, we tested for statistical differences in κ_{PLI}, κ_{MSCOH} and κ_{AEC} between subjects with education level A and B for all groups (Mann-Whitney U-test) and found no statistical differences in any group or band (see supplementary material, tables T1 to T5). MMSE scores were lower in patients with AD compared to controls ($U = 2308$, $p < 0.0001$, Mann-Whitney U-test) and MCI subjects ($U = 2193$, $p < 0.0001$, Mann-Whitney U-test). MMSE scores were also lower in MCI patients compared to controls ($U = 3517$, $p < 0.0001$, Mann-Whitney U-test).

4.2. Stability of the connectivity measures

PLI (Friedman statistics: $\chi^2(4) = 532$, $p < 0.0001$), MSCOH (Friedman statistics: $\chi^2(4) = 532$, $p < 0.0001$) and AEC (Friedman statistics: $\chi^2(4) = 447.48$, $p < 0.0001$) show a decrease in μ values as epoch length increases in all frequency bands. Dunn's test shows that all three measures stabilize at an epoch length of either 10 or 15 s in most bands. Figure 2 shows the violin plots of the distributionover all subjects of the average μ_{PLI}, μ_{MSCOH} and μ_{AEC} values for each frequency band. In the case of non-overlapping epochs, the results were similar, stabilizing at the same epoch lengths (see supplementary material, figure S1). In order for the subsequent analyses to be comparable across groups, we used 15 s epochs for all measures.

4.3. Detection of dynamic functional connectivity

Figure 3 shows the percentage of subjects as a function of the percentage of connections with statistically significant κ for PLI, leakage corrected MSCOH and leakage corrected AEC. It can be observed that leakage corrected AEC is more sensitive to the detection of dFC than leakage corrected MSCOH, which in turn is more sensitive than PLI, as a higher percentage of subjects display larger numbers of connections with dFC. In general the alpha band displays the largest number of connections with dFC for all measures. Almost 100% of subjects show connections with dFC. In the case of leakage corrected AEC, around 90% of the subjects show 5% or more connections with dFC in the alpha and beta-1 bands, and 20% of subjects show 50% or more connections with dFC. In general, controls showed the higher percentage of connections with dFC, followed by MCI patients and finally patients with AD. However, this behavior was not as marked for PLI (see supplementary material, figures S3, S4 and S5). The same analysis performed with non-overlapping epochs showed similar results for leakage corrected AEC. On the other hand, MSCOH had a lower percentage of connections with dFC when non-overlapping epochs were used, compared to overlapping epochs (see supplementary material, figure S2).

4.4. Global analyses

Figure 4 shows the grand-average κ_{PLI}, κ_{MSCOH} and κ_{AEC} values over all the connections for each frequency band after normalization. Statistically significant between-group differences ($p < 0.05$, Kruskal-Wallis test with FDR correction) were found in the alpha ($p < 0.0001$), beta-1 ($p < 0.0001$) and beta-2 ($p = 0.0399$) bands for κ_{AEC}. No statistically significant differences were found for κ_{PLI} or κ_{MSCOH}, therefore spatial between-group differences were only assessed for κ_{AEC}. In the case of non-overlapping epochs, statistically

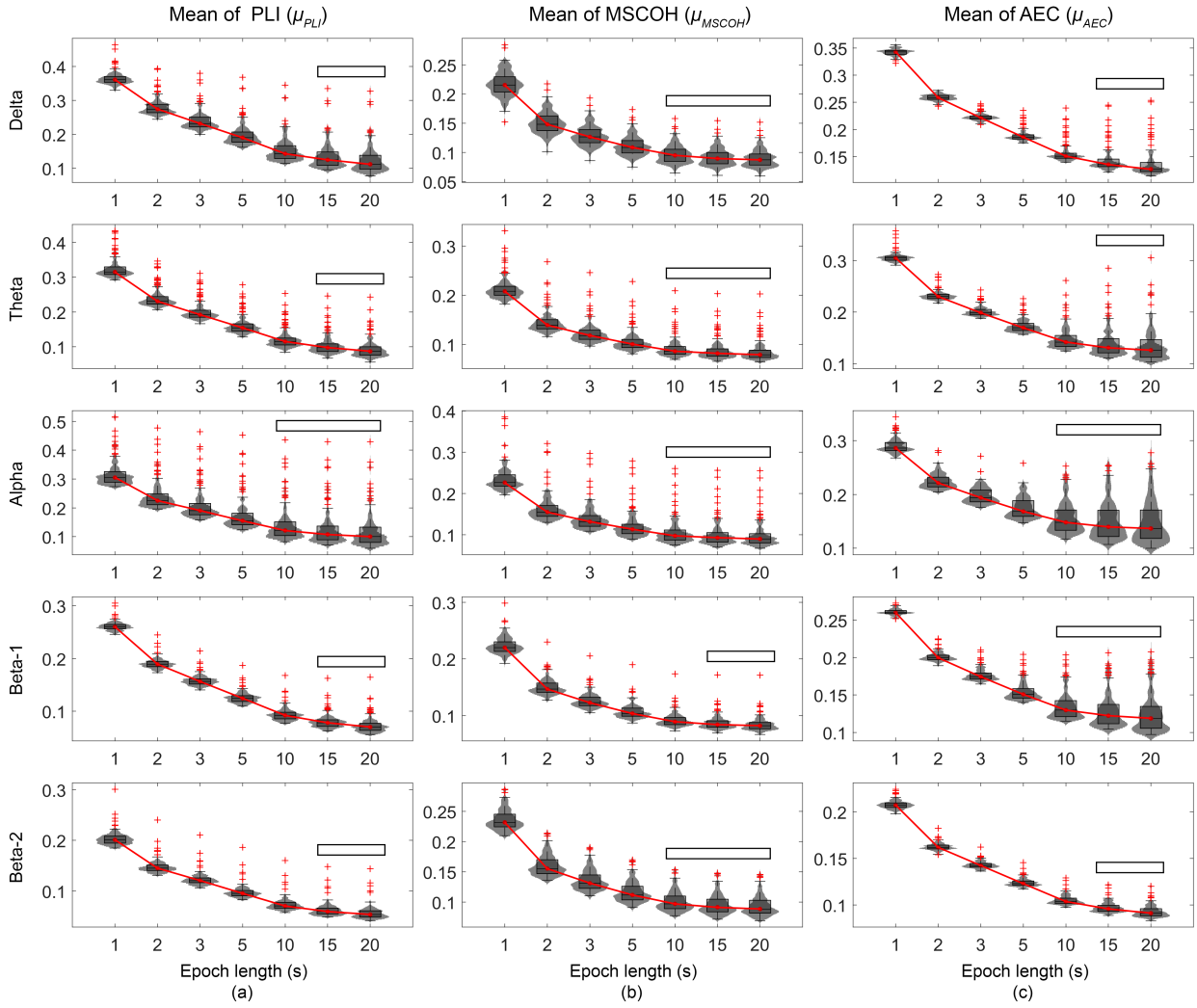

Figure 2. (a) Mean PLI (μ_{PLI}), (b) mean MSCOH (μ_{MSCOH}) and (c) mean AEC (μ_{AEC}) violin plots for each frequency band and epoch length. The red lines represent the median values and the white boxes indicate the stable epoch lengths, *i.e.* the shortest epoch length that does not show statistically significant differences with any longer ones (Dunn's multiple comparison test).

significant between-group differences ($p < 0.05$, Kruskal-Wallis test with FDR correction) were found in the alpha ($p < 0.0001$), beta-1 ($p < 0.0001$) and beta-2 ($p = 0.0217$) bands for κ_{AEC} and no differences were found for κ_{PLI} or κ_{MSCOH} (see supplementary material, figure S6). It is noteworthy that non-normalized κ_{AEC} values show similar distributions to those of normalized ones (see supplementary material figure S7).

4.5. Within- and between-group comparisons

Statistically significant ($p < 0.05$, permutation test with FDR correction) differences in κ values between regions were found for κ_{AEC}. Figure 5 shows topographic maps of the statistical differences for each pair of groups in the alpha, beta-1 and beta-2 bands. The specific p-values of the comparisons shown in figure 5 are displayed in the table T6 of the supplementary material.

In the alpha band, the patients with AD showed widespread lower κ_{AEC} than the control group. MCI subjects also showed higher κ_{AEC} than patients with AD, especially between the left and right-temporal and the central regions. Furthermore, tendencies toward lower κ_{AEC} in MCI subjects with respect to controls could also be observed. The statistical analyses in the beta-1 band also revealed a widespread κ_{AEC} decrease in patients with AD with respect to controls. MCI patients showed reduced κ_{AEC} in comparison with controls in the connections between the left-temporal and parieto-occipital regions. MCI patients also displayed higher beta-1 dFC than patients with AD, particularly in the frontal region and between the frontal and left-temporal region. Interestingly, there

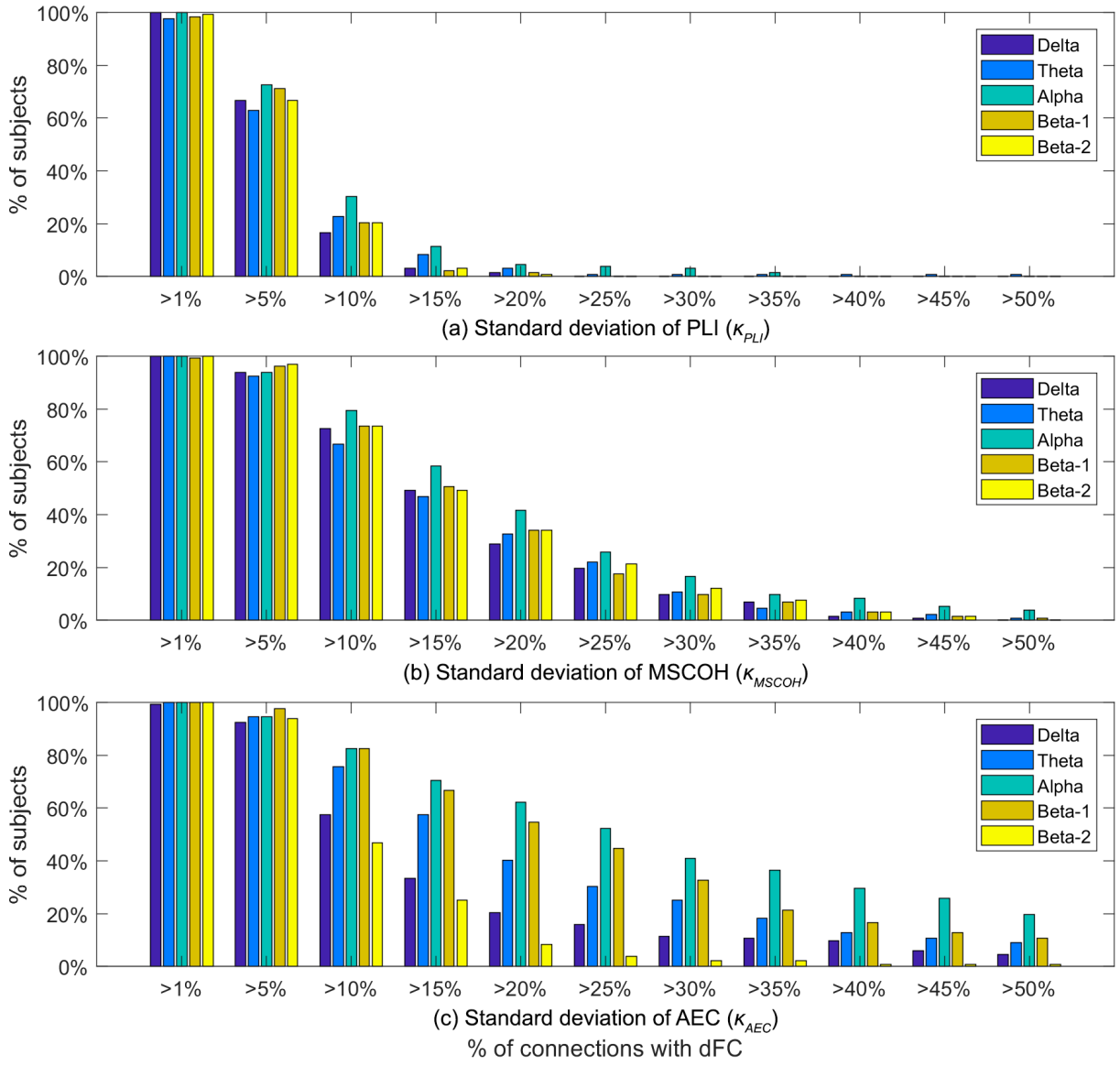

Figure 3. Percentage of subjects as a function of the percentage of connections with statistically significant (a) standard deviation of PLI (κ_{PLI}) values, (b) standard deviation of MSCOH (κ_{MSCOH}) values and (c) standard deviation of AEC (κ_{AEC}) after comparison with 500 surrogate versions of the original signals. The surrogate versions of the signals were constructed by means of the amplitude adjusted Fourier transform method (AAFT).

were more κ_{AEC} differences between MCI subjects and patients with AD than between controls and MCI subjects. In the beta-2 band, only differences between controls and patients with AD in the central and between the frontal and central regions, as well as between the central and right-temporal regions could be found.

In the case of the measures obtained with non-overlapping windows, the results were largely similar, except that the beta-2 differences between controls and patients with AD and the beta-1 differences between controls and MCI patients were slightly more statistically significant. On the other hand, the differences between MCI subjects and patients with AD in the beta-1 and alpha bands were less statistically significant (see supplementary material figure S8).

5. Discussion

In the present study, we investigated dFC in healthy controls, as well as changes in dFC in MCI and dementia due to AD. Furthermore, the effect of epoch length for three commonly used FC measures (PLI, MSCOH and AEC) was assessed in order to select

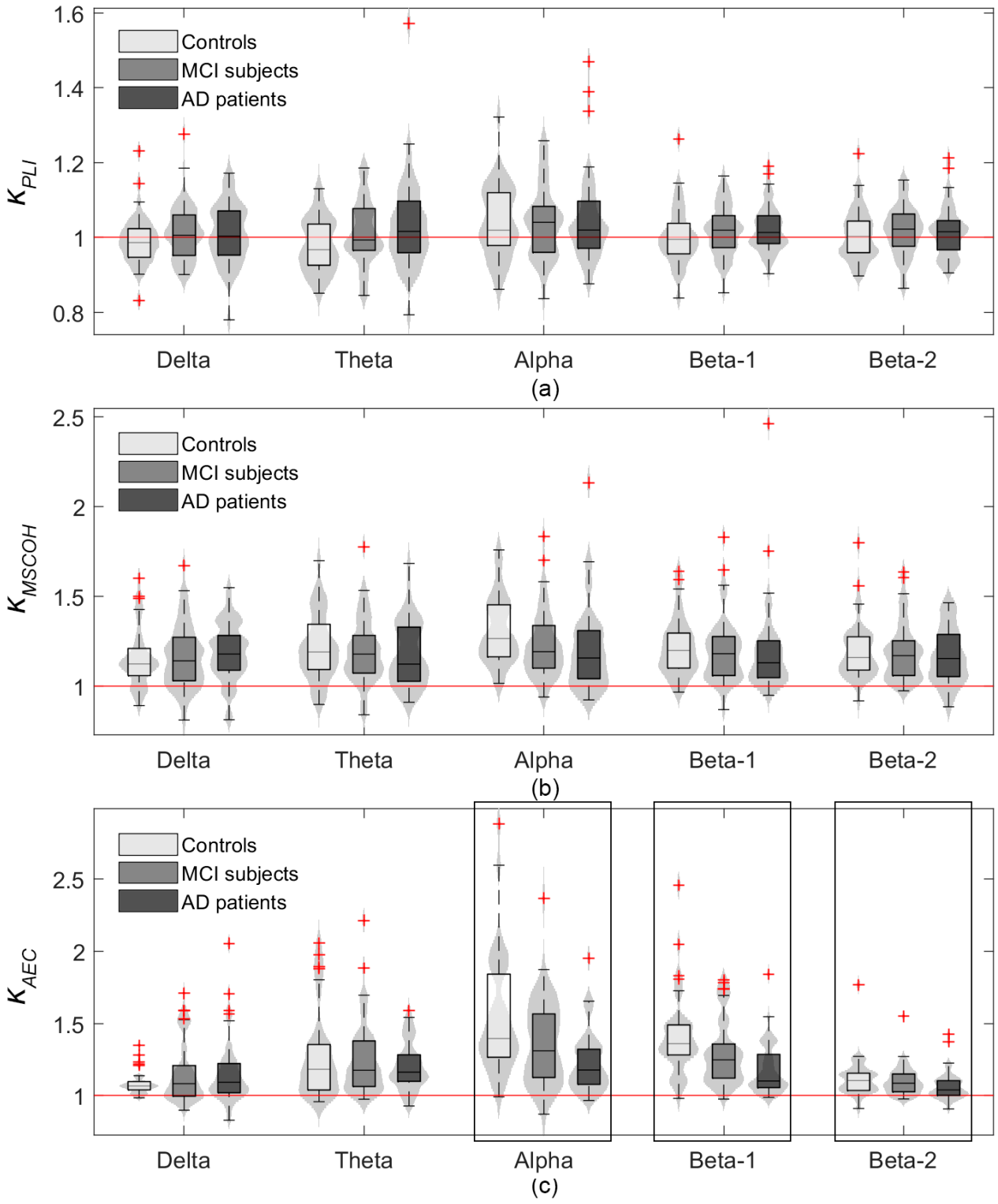

Figure 4. Violin plots depicting normalized grand-average (a) standard deviation of PLI (κ_{PLI}) values, (b) standard deviation of MSCOH (κ_{MSCOH}) values and (c) standard deviation of AEC (κ_{AEC}) values in each frequency band. The normalization was performed by dividing the raw κ values by the average κ values of the 500 surrogate versions constructed by means of amplitude adjusted Fourier transform method (AAFT). For each violin plot, the lower bar represents the first quartile, the middle bar indicates the median and the top bar marks the third quartile. The whiskers mark the most extreme points not considered outliers and the red crosses represent the outliers. Values above the red line indicate greater observed κ values for the original time series than for the surrogate versions. Statistically significant between-group differences are marked with rectangles ($p < 0.05$, Kruskal-Wallis test, FDR corrected for the number of frequency bands).

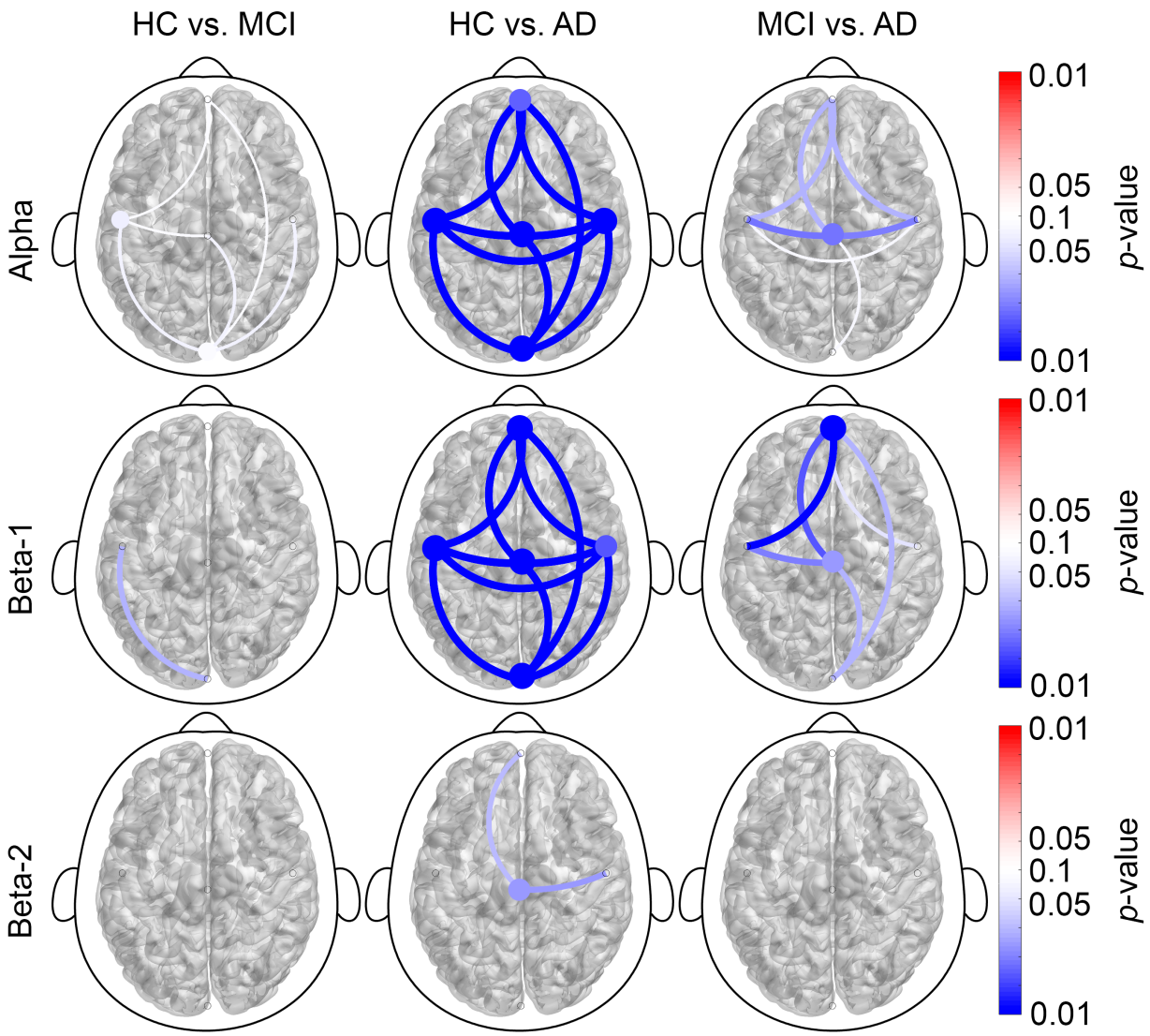

Figure 5. Spatial maps of the statistical comparisons between healthy controls and MCI subjects (HC vs. MCI), healthy controls and patients with AD (HC vs. AD) and MCI subjects versus patients with AD (MCI vs. AD) in the alpha, beta-1 and beta-2 bands for κ_{AEC}. The statistically significant pairwise comparisons between groups ($p < 0.05$, permutation test with FDR correction) are represented with blue lines if an increase in κ was found in the first group and red lines if the second group showed greater κ. Within-region differences are represented by circles, and between-region differences are indicated by lines. The specific p-values of the comparisons shown are displayed in the table T6 of the supplementary material. See figure 1 for the correspondence between EEG channels and brain regions. The brain networks were visualized with the BrainNet Viewer (http://www. nitrc.org/projects/bnv/) [42].

an appropriate epoch length for the sliding window analysis. Our findings indicate that (i) FC measures are affected by the length of the EEG epoch; (ii) dFC exists on the EEG time scale; and (iii) dFC is affected in patients with MCI and AD.

5.1. Stability of the connectivity measures

Each connectivity measure requires a different minimum epoch length to show consistent results [34]. Our results show that different connectivity measures are affected differently by epoch length, with some measures stabilizing for shorter lengths than others. A previous study found that AEC stabilized at an epoch length of 6 seconds and PLI at a length of 12 seconds [43]. In contrast, in our study PLI and AEC were found to stabilize at different epoch lengths (10 or 15 s). This might be explained by external factors, such as as the fact that we used the whole 60-second artifact-free recordings for each epoch length, while Fraschini

et al. used only the first two epochs from three 32 s segments for each epoch length and especially the fact that we performed the stability test for each frequency band separately, while Fraschini *et al.* did the test in the 1-20 Hz frequency band [43].

Our results suggest that instead of using predetermined epoch lengths, stability analyses should be performed for each connectivity measure before characterizing dFC with a sliding window approach. This way appropriate epoch lengths are used that provide stable estimates, yet are short enough to characterize fast fluctuations in functional connectivity [10]. We performed the same analyses with non-overlapping epochs and we found that the stability results were not affected by this and the results were very similar, with both measures stabilizing at the same epoch length (see supplementary material, figure S1).

5.2. Detection of dynamic functional connectivity

One of the main hypotheses of this study was that dFC can be found on the EEG time scale, while taking into account the fact that the mere presence of fluctuations in sliding window-based functional connectivity cannot be considered as evidence for its presence without an appropriate statistical test [5]. We found that evidence for dFC can indeed be found in healthy controls, MCI subjects and patients with AD, with the connectivity measure used being an influence on the observed number of dynamic connections. Furthermore, we observed that, for AEC, controls show the highest percentage of connections with dFC, followed by MCI subjects and finally patients with AD, especially in the alpha and beta-1 bands (see supplementary material, figures S3 to S5), suggesting that the progression of neurodegeneration influences the stability of FC. The connections within and between the temporal, frontal and central regions were the ones most affected in MCI and AD, with a reduction in the percentage of subjects that showed AEC dFC compared to controls (see supplementary material, figure S9). In order to reduce the chance of false positive findings, we reduced the number of statistical tests by averaging across regions [41]. Furthermore, even if a connection is not strictly dynamic after statistical testing, our proposed methodology normalizes its κ by dividing it by the average of the surrogate versions. This way, the level of dynamism that can be explained by dFC is quantified, allowing for fair between-group comparisons.

The observation that a lower number of connections with dFC were found (with the purely phased-based PLI showing the least number of connections with dFC) could suggest that amplitude-based functional connectivity is more widespread than phase-based functional connectivity. Nevertheless, failure to detect phase-based dFC could also be due to phase-based measures being more sensitive to noise fluctuations [34]. As can be seen in supplementary material figure S7, before normalization PLI shows the overall highest κ. However, after normalization this κ is almost completely eliminated, which supports the notion of phase-based measures being more sensitive to noise fluctuations. Other factors that could play a role are the use of a sliding-window approach, or the chosen length of the windows. Thus, even though only AEC shows statistically significant differences between groups, this cannot be considered evidence that there is no phase-based dFC. Still, it is worth noting that only κ_{AEC} shows higher values in controls and MCI patients with respect to patients with AD even before normalization (see supplementary material, figure S7).

5.3. Specific MCI- and AD-related dFC patterns

Statistically significant differences between groups κ_{AEC} were found in the alpha and beta-1 bands (and to a lesser extent in the beta-2 band). No differences were found for κ_{PLI} or κ_{MSCOH}. The results for κ_{AEC} suggest that dFC is affected by AD and MCI, with a loss of stability in coupling being present in both groups. Viewing AD as a disconnection syndrome, it is to be expected that AD connectivity patterns will be more abnormal along the progression of the disease [20]. This is indeed the case, with the grand-average κ_{AEC} values showing a clear tendency towards a reduction in dFC for MCI subjects, as well as a more pronounced κ_{AEC} decrease in patients with AD in the alpha, beta-1 and beta-2 bands.

In the alpha band, differences in dFC were only found between healthy controls and patients with AD for κ_{AEC}. It has been widely reported that AD is associated with a decrease in alpha band power [1, 45], as well as with a loss of functional connectivity [46, 47]. Our results suggest that a decrease in dFC is also present in AD. Hence, not only is FC reduced in AD, but it also more sluggish, evolving at a slower rate than for control subjects. This could mean that the disconnection hypothesis in sFC could be extended to the dFC domain [47]. Given that only non-statistically significant tendencies towards less dFC in MCI patients compared to controls were found in this band, this suggests that MCI dFC in the alpha band is not as abnormal as in AD. This finding could imply that a less dynamic FC system is a sign of AD that is not present in MCI, as opposed to the static functional disconnection that is already present in MCI and that becomes more marked in AD [1, 24].

Widespread statistically significant differences between controls and patients with AD were also found in the beta-1 band, with controls showing higher normalized κ_{AEC} between all regional pairs. Interestingly, there were some tendencies towards lower

normalized κ_{AEC} in MCI subjects compared to healthy controls (more marked with non-overlapping windows, see supplementary material figure S8), which suggests that beta-1 dFC might deteriorate earlier in the aging-MCI-AD continuum than alpha dFC. Like in the alpha band, statistically significant differences in variablity were more marked between MCI patients and patients with AD than between controls and MCI patients, further suggesting that dFC might be altered at a later stage in the MCI-AD continuum. Previous studies found early alterations of sFC in the beta band. In particular, Gómez *et al.* found both inter- and intra-hemisferic decrements in Granger Causality connectivity for MCI subjects when compared to controls [48]. Babiloni *et al.* found parietal to frontal direction of the information flux to be weaker in MCI subjects and patients with AD when compared to controls [49]. Our findings thus support the notion of MCI being a prodromal stage of AD. The beta band has been traditionally associated with sensorimotor functions. However, it has recently been implicated in the preservation of the current brain state [50]. It is one of the less studied frequency bands when it comes to AD and MCI [51], but some studies suggest that it could have a special significance in the early stages of AD, with a loss of beta band synchronization reflecting the specific pathology in AD, as opposed to being simply due to aging [46]. Furthermore, given that one of the most documented alterations in EEG oscillations in AD and MCI is a shift of the power spectrum towards lower frequencies (theta and delta) [52], a decrease in EEG connectivity stability could be expected for higher frequency bands. Indeed, we found positive correlation between normalized κ_{AEC} and relative power in patients with AD and especially in MCI patients in the beta-1 band (see supplementary material, figure S10), but no correlation was found for controls. A correlation between sFC and average power was previously found by de Haan *et al.* using computational modeling [53]. Our results might indicate that this correlation between average power and connectivity could be extended to dFC, perhaps suggesting that the high correlation between relative power and κ_{AEC} in MCI patients in the beta-1 band is pathological and related to high activity levels that could lead to neuronal damage [53].

The reduction in dFC found in patients with AD was specially prevalent in the connections between the left-temporal, frontal and central regions. Reductions in sFC for AD patients in these regions have been found in various MEG-based studies [18]. In particular, the long range sFC connections between the left hemisphere and other regions seem more affected by AD according to these studies [18], which agrees with our results in the beta-1 band (see supplementary material, figure S11). Our results suggest that this might also be the case for beta-1 dFC, as the connections involving the left hemisphere were reduced significantly in patients with AD compared to patients with MCI. This could suggest that the left hemisphere is more affected than other regions during the development of AD. Indeed, an MEG-based eyes-closed resting-state study found reduced beta standard deviation (SD) of local activity in patients with AD compared to elderly controls in the left hemisphere [47]. This may indicate that a reduction in local activation may be related to a loss of dFC between the areas affected.

Our findings indicate that dFC decreases in the alpha, beta-1 and beta-2 bands for AD subjects, which would mean that not only is sFC altered in AD (see supplementary material, figure S11) [20], but dFC is as well. Furthermore, the altered beta-1 dFC in MCI supports both the notion of MCI as a disconnection syndrome, as well as MCI and AD being on a continuum. The fact that alterations in EEG dFC were only found in three frequency bands supports the view that cognitive disturbances associated with AD may not be solely a product of the loss of neurons, but also due to impairments in the temporal coordination of distributed neuronal activity [52]. A fMRI dFC study suggested that the static functional connectivity abnormalities that have been found in resting-state AD could be due to the varying dwell time in specific modular configurations, rather than static connectivity magnitude [21]. The decrease in alpha and beta-1 dFC could be due to the alterations of GABAergic receptor subunits, the depression of cholinergic inhibitory activity, the decrease in inhibitory neurotransmission or the enhancement of excitatory glutamatergic receptor activity, all of which could result in desynchronization of neuronal activity [54]. This desynchronization could cause a loss in coupling strength, which has been associated, by means of network modeling, with a stable spontaneous non-fluctuating state characterized by low-level firing activity in all areas of the brain [27]. In contrast, healthy resting-state networks operate at an optimal working point (point of criticality) characterized by a loss of stability in the aforementioned trivial state and the appearance of new multistable states, with transitions occurring between them. [27]. This lack of state switching could explain the reduced dFC found in patients with MCI and AD. This theory is supported by our findings of widespread μ_{AEC} differences between groups (see supplementary material, figure S11), with patients with MCI and AD showing reduced sFC between the regions where a dFC decrease was found in the alpha, beta-1 and beta-2 bands.

5.4. Limitations and future research lines

This study has several limitations that merit further attention. Firstly, all connectivity estimates were made at the sensor level, which does not allow to make inferences about the interactions between anatomical regions [55]. Future studies should address this by performing computations at the source level to localize the brain areas where dFC is affected by MCI and AD with higher accuracy. However, it has been found that there is a strong correlation between scalp- and source-level global mean connectivity for leakage corrected AEC [55], which suggests that our findings could be independent of the approach used.

Secondly, even though AEC was corrected for leakage effects by means of orthogonalization, this method does not eliminate all possible leakage effects. This would require the raw data to be Gaussian distributed, which might not be true, as well as assuming that the signal-to-noise ratio is constant across time and frequency [10]. However, we tried to maximize the effectiveness of the leakage reduction by performing it after bandpass filtering the data, and for every epoch separately, as opposed to the whole data set [10].

In this study, the sliding window approach was used to characterize dFC. Although it has been widely used in fMRI dFC studies [56], it is not without limitations. We tried to address the common problem of choosing window length [10] by performing a stability test to eliminate bias. However, ideally the window width should be chosen to match the timescale of the underlying fluctuations, which are *a-priori* unknown [10]. Furthermore, the sliding window has reduced temporal resolution (e.g. a connectivity event could be detected in several overlapping time-windows if they are too large). Some alternatives to the sliding window, such as the wavelet transform or using data-driven variable epoch lengths by means of Hidden Markov Models have been proposed [10], which could be used in future studies.

We have considered the results of the study to be supportive of the MCI-AD continuum hypothesis. It is important to note, however, the fact that there is no information of the evolution of the subjects from MCI to AD must be taken into consideration. It might be the case that the middle ground behavior found in the MCI group could be indicative of two subgroups, one closer to control-like behavior and one closer to AD, depending on the evolution towards AD or not. Thus, other possible explanations must be considered and further research would need to be conducted with information regarding the evolution of MCI patients towards AD to arrive at a definitive conclusion.

Finally, it has been shown that rejecting the null hypothesis with the phase randomization method of constructing surrogate data does not necessarily mean that there is dFC, but could also be due to non linearity and/or non-Gaussianity [57]. Thus, in order to control for non-Gaussianity, we used AAFT, which matches the amplitude distribution of the original data [57]. Nevertheless, understanding the results of statistical testing for dFC is not trivial and alternative interpretations should always be considered. Future investigations could explore the possibility of using autoregressive randomization models to explore the dynamic properties of EEG data [57].

To our knowledge, this is the first study to address EEG dFC in AD and MCI, and our findings suggest that this could be an interesting research line for future studies that could characterize it with a more in-depth approach, such as identifying repeating patterns of connectivity. Indeed, a few fMRI studies used this approach, based on the assumption that connectivity patterns can be categorized into a number of defined states [2, 10]. Possible approaches that could be used are K-means clustering and Independent Component Analysis [10].

6. Conclusion

This study proposed the application of dFC techniques to the study of AD and MCI using resting-state EEG recordings. Our results suggest that dFC can be found at the EEG time scale. The results also support the notion that the choice of window length is vital when using a sliding window approach to detect dFC in order to eliminate effects of instability not due to intrinsic EEG dynamism. Furthermore, the abnormal dFC for patients with AD and, to a lesser extent, MCI subjects, particularly in the beta-1 band, supports the notion of AD resting-state networks operating at a point below criticality due to reduced coupling strength, which is supported by the lower sFC observed in MCI and AD. This could explain the lower dFC as being due to fewer transitions between network states, which may indicate that the neural system is operating at a state of low firing activity in many cortical areas. This is the main research line that we want to address in future studies, as we hypothesize that the lower κ_{AEC} in AD versus controls could be a sign of decreased network state switching in AD subjects compared to controls.

Furthermore, it also supports the notion of the MCI-AD continuum, as patients with MCI showed higher dFC than patients with AD, but lower than controls. If this hypothesis could be confirmed, it would mean that dFC measures such as κ_{AEC} could potentially be used as biomarkers for AD although further research is needed, including classification studies with different databases, as well as information regarding the evolution of MCI patients towards AD.

Finally, the observation that MCI patients showed a higher level dFC than patients with AD in the alpha and beta-1 bands, coupled with the statistically significant correlation between relative power and dFC in the latter band for MCI patients could be indicative of pathologically high levels of neuronal activity that may lead to neuronal damage and a loss of dFC in AD.

7. Acknowledgements

This research was supported by 'European Commission' and 'European Regional Development Fund' (FEDER) under project 'Análisis y correlación entre el genoma completo y la actividad cerebral para la ayuda en el diagnóstico de la enfermedad de Alzheimer' ('Cooperation Programme Interreg V-A Spain-Portugal, POCTEP 2014-2020'), and by 'Ministerio de Ciencia, Innovación y Universidades' and FEDER under projects PGC2018-098214-A-I00 and DPI2017-84280-R. P. Núñez was in receipt of a predoctoral scholarship 'Ayuda para contratos predoctorales para la Formación de Profesorado Universitario (FPU)' grant from the 'Ministerio de Educación, Cultura y Deporte' (FPU17/00850).

References

[1] Babiloni C, Lizio R, Marzano N, Capotosto P, Soricelli A, Triggiani A I, Cordone S, Gesualdo L and Del Percio C 2015 *International Journal of Psychophysiology* **103** 88–102 ISSN 18727697 URL http://dx.doi.org/10.1016/j.ijpsycho.2015.02.008

[2] Hutchison R M, Womelsdorf T, Allen E A, Bandettini P A, Calhoun V D, Corbetta M, Della Penna S, Duyn J H, Glover G H, Gonzalez-Castillo J, Handwerker D A, Keilholz S, Kiviniemi V, Leopold D A, de Pasquale F, Sporns O, Walter M and Chang C 2013 *NeuroImage* **80** 360–378 ISSN 10538119 (*Preprint* NIHMS150003) URL http://dx.doi.org/10.1016/j.neuroimage.2013.05.079

[3] Friston K J 1994 *Human Brain Mapping* **2** 56–78 ISSN 1097-0193

[4] Friston K J 2011 *Brain Connectivity* **1** 13–36 ISSN 2158-0014 URL http://www.liebertonline.com/doi/abs/10.1089/brain.2011.0008

[5] Hindriks R, Adhikari M H, Murayama Y, Ganzetti M, Mantini D, Logothetis N K and Deco G 2016 *NeuroImage* **127** 242–256 ISSN 10959572 URL http://dx.doi.org/10.1016/j.neuroimage.2015.11.055

[6] Hansen E C A, Battaglia D, Spiegler A, Deco G and Jirsa V K 2015 *NeuroImage* **105** 525–535 ISSN 10959572 URL http://dx.doi.org/10.1016/j.neuroimage.2014.11.001

[7] Allen E A, Damaraju E, Eichele T, Wu L and Calhoun V D 2017 *Brain topography* **0** 1–16 ISSN 1573-6792 URL http://link.springer.com/10.1007/s10548-017-0546-2http://www.ncbi.nlm.nih.gov/pubmed/28229308http://www.pubmedcentral.nih.gov/articlerender.fcgi?artid=PMC5568463

[8] Chang C and Glover G H 2010 *NeuroImage* **50** 81–98 ISSN 10538119 URL http://dx.doi.org/10.1016/j.neuroimage.2009.12.011

[9] Poza J, Gómez C, García M, Tola-Arribas M A, Carreres A, Cano M and Hornero R 2017 *Current Alzheimer Research* **14** 924–936

[10] O'Neill G C, Tewarie P, Vidaurre D, Liuzzi L, Woolrich M W and Brookes M J 2017 *NeuroImage* 1–18 ISSN 10959572 URL https://doi.org/10.1016/j.neuroimage.2017.10.003

[11] Mantini D, Perrucci M G, Del Gratta C, Romani G L and Corbetta M 2007 *Proceedings of the National Academy of Sciences of the United States of America* **104** 13170–5 ISSN 0027-8424 URL http://www.pubmedcentral.nih.gov/articlerender.fcgi?artid=1941820{&}tool=pmcentrez{&}rendertype=abstract

[12] Mayhew S and Bagshaw A 2017 *NeuroImage* **155** 120–137 ISSN 10538119 URL http://www.sciencedirect.com/science/article/pii/S1053811917303695

[13] Britz J, Van De Ville D and Michel C M 2010 *NeuroImage* **52** 1162–1170 ISSN 10538119 URL http://dx.doi.org/10.1016/j.neuroimage.2010.02.052

[14] Kabbara A, EL Falou W, Khalil M, Wendling F and Hassan M 2017 *Scientific Reports* **7** 2936 ISSN 2045-2322 URL http://www.nature.com/articles/s41598-017-03420-6

[15] Carbo E W, Hillebrand A, Van Dellen E, Tewarie P, De Witt Hamer P C, Baayen J C, Klein M, Geurts J J, Reijneveld J C, Stam C J and Douw L 2017 *Scientific Reports* **7** 1–10 ISSN 20452322 URL http://dx.doi.org/10.1038/srep42117

[16] Pievani M, de Haan W, Wu T, Seeley W W and Frisoni G B 2011 *The Lancet Neurology* **10** 829–843 ISSN 14744422

[17] Palop J and Mucke L 2010 *Nature neuroscience* **13** 812–818 ISSN 1546-1726

[18] Engels M M, van der Flier W M, Stam C J, Hillebrand A, Scheltens P and van Straaten E C 2017 *Clinical Neurophysiology* **128** 1426–1437 ISSN 18728952 URL http://dx.doi.org/10.1016/j.clinph.2017.05.012

[19] Babiloni C, Del Percio C, Lizio R, Noce G, Lopez S, Soricelli A, Ferri R, Pascarelli M T, Catania V, Nobili F, Arnaldi D, Famà F, Aarsland D, Orzi F, Buttinelli C, Giubilei F, Onofrj M, Stocchi F, Vacca L, Stirpe P, Fuhr P, Gschwandtner U, Ransmayr G, Garn H, Fraioli L, Pievani M, Frisoni G B, D'Antonio F, De Lena C, Güntekin B, Hanoğlu L, Başar E, Yener G, Emek-Savaş D D, Triggiani A I, Franciotti R, Taylor J P, De Pandis M F and Bonanni L 2018 *Journal of Alzheimer's Disease* **62** 247–268 ISSN 13872877 URL http://www.medra.org/servlet/aliasResolver?alias=iospress{&}doi=10.3233/JAD-170703

[20] Bokde A L W, Ewers M and Hampel H 2009 *Progress in Neurobiology* **89** 125–133 ISSN 03010082

[21] Jones D T, Vemuri P, Murphy M C, Gunter J L, Senjem M L, Machulda M M, Przybelski S A, Gregg B E, Kantarci K, Knopman D S, Boeve B F, Petersen R C and Jack C R 2012 *PLoS ONE* **7** ISSN 19326203

[22] Petersen R C 2004 *Archives of Neurology* **62** 1160–1163; discussion 1167 ISSN 0003-9942

[23] Gómez C, Stam C J, Hornero R, Fernández A and Maestú F 2009 *IEEE Transactions on Biomedical Engineering* **56** 1683–1690 ISSN 1558-2531 URL http://www.ncbi.nlm.nih.gov/pubmed/19362905

[24] Tóth B, File B, Boha R, Kardos Z, Hidasi Z, Gaál Z A, Csibri É, Salacz P, Stam C J and Molnár M 2014 *International Journal of Psychophysiology* **92** 1–7 ISSN 01678760

[25] Babiloni C, Ferri R, Binetti G, Cassarino A, Forno G D, Ercolani M, Ferreri F, Frisoni G B, Lanuzza B, Miniussi C, Nobili F, Rodriguez G, Rundo F, Stam C J, Musha T, Vecchio F and Rossini P M 2006 *Brain Research Bulletin* **69** 63–73 ISSN 03619230

[26] Núñez P, Poza J, Gómez C, Ruiz-Gómez S J, Rodríguez-

González V, Tola-Arribas M A, Cano M and Hornero R 2018 Analysis Electroencephalographic Dynamic Functional Connectivity in Alzheimer's Disease *World Congress on Medical Physics and Biomedical Engineering 2018. IFMBE Proceedings* vol 68/2 ed Lhotska L, Sukupova L, Lacković I and Ibbott G (Singapore: Springer) pp 165–168 URL https://link.springer.com/chapter/10.1007/978-981-10-9038-7{_}30

[27] Deco G, Jirsa V K and McIntosh A R 2013 *Trends in Neurosciences* **36** 268–274 ISSN 01662236 URL http://dx.doi.org/10.1016/j.tins.2013.03.001

[28] McKhann G, Knopman D S, Chertkow H, Hymann B, Jack C R, Kawas C, Klunk W, Koroshetz W, Manly J, Mayeux R, Mohs R, Morris J, Rossor M, Scheltens P, Carrillo M, Weintrub S and Phelphs C 2011 *Alzheimers Dementia* **7** 263–269 ISSN 1552-5279 (*Preprint* NIHMS150003)

[29] Albert M S, DeKosky S T, Dickson D, Dubois B, Feldman H H, Fox N C, Gamst A, Holtzman D M, Jagust W J, Petersen R C, Snyder P J, Carrillo M C, Thies B and Phelps C H 2011 *Alzheimer's and Dementia* **7** 270–279 ISSN 15525260 (*Preprint* NIHMS150003) URL http://dx.doi.org/10.1016/j.jalz.2011.03.008

[30] Roach B J and Mathalon D H 2008 *Schizophrenia Bulletin* **34** 907–926 ISSN 05867614

[31] Stam C J, Nolte G and Daffertshofer A 2007 *Human Brain Mapping* **28** 1178–1193 ISSN 10659471

[32] O'Neill G C, Barratt E L, Hunt B a E, Tewarie P K and Brookes M J 2015 *Physics in Medicine and Biology* **60** R271–R295 ISSN 0031-9155 URL http://iopscience.iop.org/article/10.1088/0031-9155/60/21/R271{%}5Cnhttp://stacks.iop.org/0031-9155/60/i=21/a=R271?key=crossref.459527ecaf4b58204b45236cde39bfc4

[33] Bastos A M and Schoffelen J M 2016 *Frontiers in Systems Neuroscience* **9** 1–23 ISSN 1662-5137 URL http://journal.frontiersin.org/article/10.3389/fnsys.2015.00175/abstract

[34] Colclough G, Woolrich M, Tewarie P, Brookes M, Quinn A and Smith S 2016 *NeuroImage* **138** 284–293 ISSN 10538119 URL http://linkinghub.elsevier.com/retrieve/pii/S1053811916301914

[35] Brookes M J, Hale J R, Zumer J M, Stevenson C M, Francis S T, Barnes G R, Owen J P, Morris P G and Nagarajan S S 2011 *NeuroImage* **56** 1082–1104 ISSN 10538119 URL http://dx.doi.org/10.1016/j.neuroimage.2011.02.054

[36] Brookes M J, O'Neill G C, Hall E L, Woolrich M W, Baker A, Palazzo Corner S, Robson S E, Morris P G and Barnes G R 2014 *NeuroImage* **91** 282–299 ISSN 10538119

[37] Bachiller A, Díez A, Suazo V, Domínguez C, Ayuso M, Hornero R, Poza J and Molina V 2014 *European Archives of Psychiatry and Clinical Neuroscience* **264** 533–543 ISSN 14338491

[38] Theiler J, Eubank S, Longtin A, Galdrikian B and Doyne Farmer J 1992 *Physica D: Nonlinear Phenomena* **58** 77–94 ISSN 01672789 (*Preprint* 9909037)

[39] Prichard D and Theiler J 1994 *Physical Review Letters* **73** 951–954 ISSN 19357001

[40] Khambhati A N, Sizemore A E, Betzel R F and Bassett D S 2017 *NeuroImage* 1–13 ISSN 10959572 URL http://dx.doi.org/10.1016/j.neuroimage.2017.06.029

[41] Stam C J, Jones B F, Manshanden I, van Cappellen van Walsum A M, Montez T, Verbunt J P, de Munck J C, van Dijk B W, Berendse H W and Scheltens P 2006 *NeuroImage* **32** 1335–1344 ISSN 10538119

[42] Xia M, Wang J and He Y 2013 *PLoS ONE* **8** ISSN 19326203

[43] Fraschini M, Demuru M, Crobe A, Marrosu F, Stam C J and Hillebrand A 2016 *Journal of Neural Engineering* **13** 036015 ISSN 1741-2552 (*Preprint* 1606.02840) URL http://www.ncbi.nlm.nih.gov/pubmed/27137952

[44] Benjamini Y and Hochberg Y 1995 *Journal of the Royal Statistical Society* **57** 289–300 ISSN 00359246 (*Preprint* 95/57289)

[45] Poza J, Hornero R, Abásolo D, Fernández A and García M 2007 *Medical Engineering and Physics* **29** 1073–1083 ISSN 13504533

[46] Stam C J, Van Der Made Y, Pijnenburg Y A L and Scheltens P 2003 *Acta Neurologica Scandinavica* **108** 90–96 ISSN 00016314

[47] Koelewijn L, Bompas A, Tales A, Brookes M J, Muthukumaraswamy S D, Bayer A and Singh K D 2017 *Clinical Neurophysiology* **128** 2347–2357 ISSN 18728952 URL https://doi.org/10.1016/j.clinph.2017.04.018

[48] Gómez C, Juan-Cruz C, Poza J, Ruiz-Gómez S J, Gomez-Pilar J, Núñez P, García M, Fernández A and Hornero R 2017 *Journal of Alzheimer's Disease* **Preprint** 1–12 ISSN 13872877 URL http://www.medra.org/servlet/aliasResolver?alias=iospress{&}doi=10.3233/JAD-170475

[49] Babiloni C, Ferri R, Binetti G, Vecchio F, Frisoni G B, Lanuzza B, Miniussi C, Nobili F, Rodriguez G, Rundo F, Cassarino A, Infarinato F, Cassetta E, Salinari S, Eusebi F and Rossini P M 2009 *Neurobiology of Aging* **30** 93–102 ISSN 01974580

[50] Spitzer B and Haegens S 2017 *Eneuro* **4** ENEURO.0170–17.2017 ISSN 2373-2822 URL http://eneuro.sfn.org/lookup/doi/10.1523/ENEURO.0170-17.2017

[51] Güntekin B, Emek-Savaş D D, Kurt P, Yener G G and Başar E 2013 *NeuroImage: Clinical* **3** 39–46 ISSN 22131582

[52] Uhlhaas P J and Singer W 2006 *Neuron* **52** 155–168 ISSN 08966273

[53] de Haan W, Mott K, van Straaten E C, Scheltens P and Stam C J 2012 *PLoS Computational Biology* **8** ISSN 1553734X (*Preprint* journal.pcbi.1002582)

[54] Babiloni C, Del Percio C, Boccardi M, Lizio R, Lopez S, Carducci F, Marzano N, Soricelli A, Ferri R, Triggiani A I, Prestia A, Salinari S, Rasser P E, Basar E, Famà F, Nobili F, Yener G, Emek-Savaş D D, Gesualdo L, Mundi C, Thompson P M, Rossini P M and Frisoni G B 2015 *Neurobiology of Aging* **36** 556–570 ISSN 15581497

[55] Lai M, Demuru M, Hillebrand A and Fraschini M 2018 *Scientific Reports* **8** 1–8 ISSN 20452322 URL http://dx.doi.org/10.1038/s41598-018-30869-w

[56] Handwerker D A, Roopchansingh V, Gonzalez-Castillo J and Bandettini P A 2012 *NeuroImage* **63** 1712–1719 ISSN 10538119 (*Preprint* NIHMS150003) URL http://dx.doi.org/10.1016/j.neuroimage.2012.06.078

[57] Liégeois R, Laumann T O, Snyder A Z, Zhou J and Yeo B T 2017 *NeuroImage* **163** 437–455 ISSN 10959572 (*Preprint* 135681)